Biophysical Journal

**Supporting Material**

# Segregated Phases In Pulmonary Surfactant Membranes Do Not Show Coexistence Of Lipid Populations With Differentiated Dynamic Properties

Jorge Bernardino de la Serna, Greger Oradd, Luis Bagatolli, Adam C. Simonsen, Derek Marsh, Goran Lindblom, and Jesus Perez-Gil

**Supplementary Table 1**

**Lateral diffusion coefficient ($D_L$) of phospholipids in membranes reconstituted from different fractions of pulmonary surfactant, as determined by pulsed field gradient NMR.**

| | $D_L$ ($\mu m^2 s^{-1}$)* | | | |
|---|---|---|---|---|
| | **25°C** | **30°C** | **35°C** | **40°C** |
| **NPSE** | 1.53 | 2.86 | 5.37 | 7.62 |
| **NPSL** | 1.45 | 3.35 | 5.90 | 8.59 |
| **NPSP** | 2.45 | 3.85 | 6.36 | 9.56 |

* The absolute error in the measurements is typically ±0.5 □$m^2$/s.

**Supplementary Figure 1**

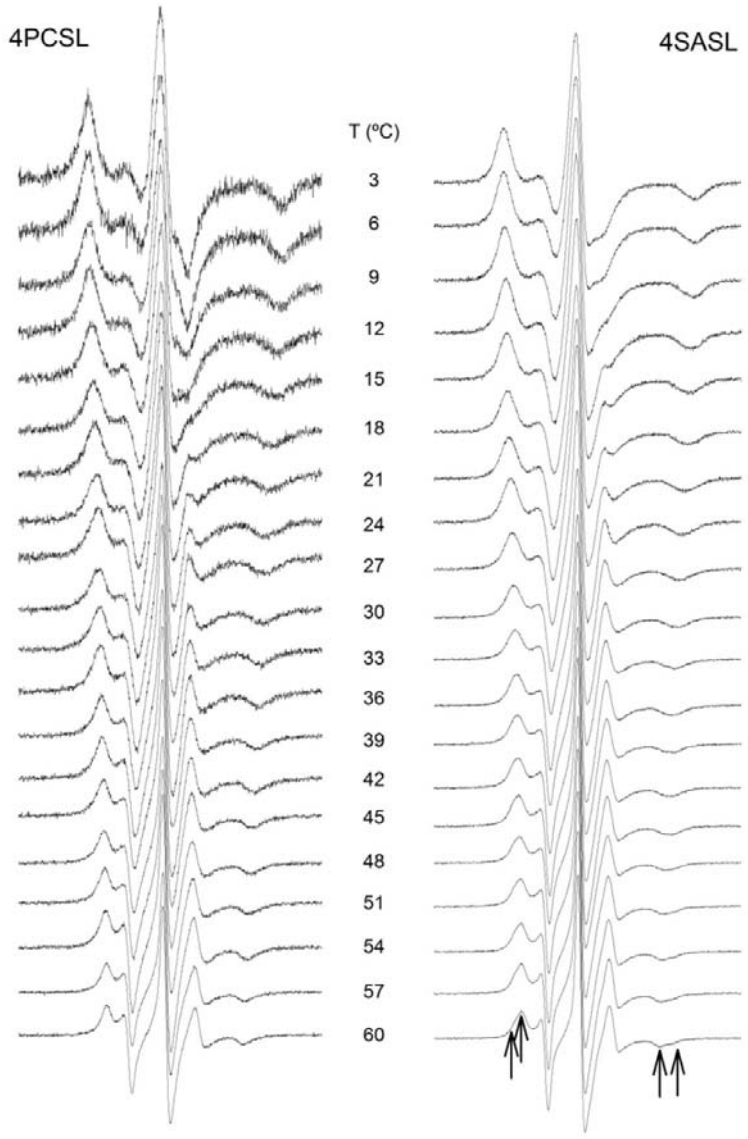


**Temperature dependence of the mobility of phospholipid acyl chains in native pulmonary surfactant membranes, determined by electron paramagnetic resonance (EPR) spectroscopy**

Suspensions of native pulmonary surfactant were spin-labeled by incubation with 1% mol/mol with respect to phospholipid of either stearic acid bearing a nitroxide spin group on the 4$^{th}$ carbon of the chain (4-SASL) or a phosphatidylcholine probe esterified at the *sn*-2 position with 4-SASL (4-PCSL). EPR spectra were recorded at the temperatures indicated. The arrows in the 4-SASL spectra at high temperature indicate the simultaneous presence of components from protonated and unprotonated forms of the fatty acid spin probe.

**Supplementary Figure 2**

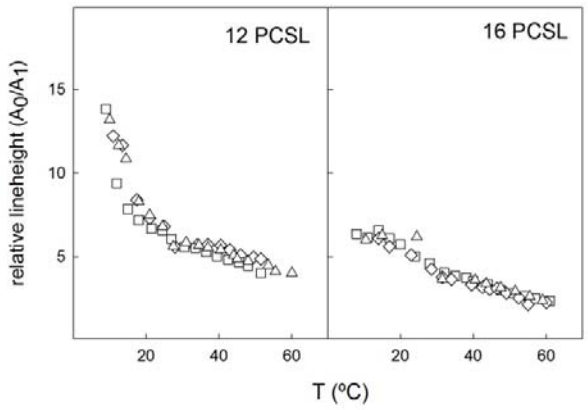


**Temperature dependence of the mobility of segments deep in the phospholipid acyl chains in native pulmonary surfactant and membranes reconstituted from its fractions**

Relative linehights $A_0/A_1$, of central to low-field peak in the EPR spectra of native surfactant (NPS, ○) or its reconstituted fractions (NPSE, □; NPSL, ◊; NPSP, Δ), as a function of temperature, for samples containing phosphatidylcholine probes spin-labelled at the 12- or 16-positions (12-PCSL or 16-PCSL, respectively) of the *sn*-2 acyl chain.

**Supplementary Figure 3**

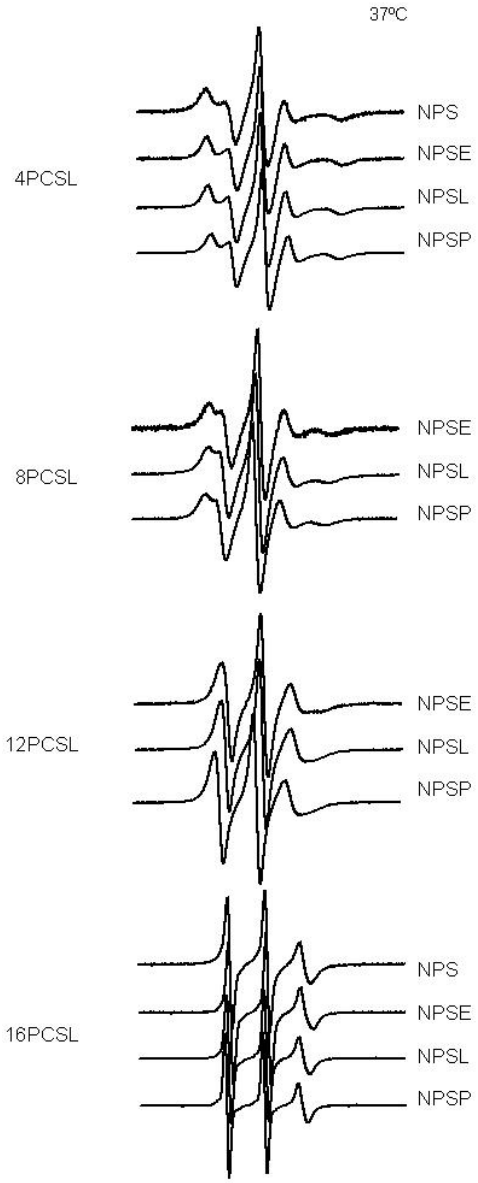


**Dynamics of different segments of the phospholipid acyl chains in native pulmonary surfactant and membranes reconstituted from its fractions, at 37°C**

EPR spectra of native surfactant (NPS) or its reconstituted fractions (NPSE, NPSL, NPSP), doped with phosphatidylcholine probes spin labelled at C-atom position *n* in the *sn*-2 chain (*n*-PCSL), at 37°C.

**Supplementary Figure 4**

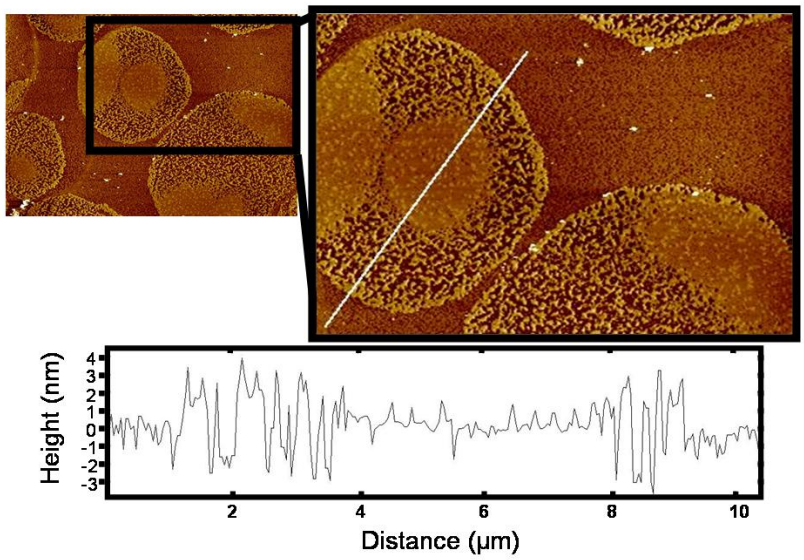


**Nanostructure of native pulmonary surfactant membranes**

Surface topology at the nanometer scale of supported native pulmonary surfactant membranes, prepared by the Langmuir-Blodgett (LB) technique, and scanned by atomic force microscopy (AFM). Lower panel plots the height profile corresponding to the white line in the right image.

Supported bilayers of NPS were prepared as described previously (Bernardino de la Serna et al., J. Biol. Chem. 2004, 279, 40715) by spreading aqueous NPS suspensions on an ultrapure water subphase in a Langmuir-Blodgett trough (Kibron, μ-trough) at a surface pressure of 1 mN/m. After 10 min equilibration, the film was compressed to 40 mN/m and transferred to a freshly cleaved muscovite mica substrate (Plano, Wetzlar, Germany), previously immersed into the subphase, at a constant speed of 1.5 mm/min. Following the initial deposition, a second layer was transferred onto the first by re-immersion of the coated mica into the subphase at 1.5 mm/s (also at a constant pressure of 40 mN/m). The supported membranes used in the AFM experiments are thus bilayer structures formed by double transfer of the surface film. AFM images were obtained under aqueous conditions in a PicoSPM (Molecular Imaging, Tempe, AZ) microscope operated in the magnetic tapping mode (MAC) using MAC levers operated around their resonance frequency of 25 kHz (in water) with a force constant of $k_{\mathrm{MAClever}}$ = 2.8 N/m (nominal). The scan rate used for imaging was in the range of 1.2–1.9 Hz for all cases.